EurJIC European Journal of Inorganic Chemistry

A Journal of ChemPubSoc Europe

Accepted Article

Title: Single-Ion Magnets Based on Mononuclear Cobalt (II) Complexes with Sulfadiazine.

Authors: Cristian Villa-Pérez; Itziar Oyarzabal; Gustavo Alberto Echeverría; Gloria Cristina Valencia-Uribe; José Manuel Seco; Delia Beatriz Soria

To be cited as: Eur. J. Inorg. Chem. 10.1002/ejic.201600777

Link to VoR: http://dx.doi.org/10.1002/ejic.201600777

WILEY-VCH

Single-Ion Magnets Based on Mononuclear Cobalt (II) Complexes with Sulfadiazine.

Cristian Villa-Pérez[1], Itziar Oyarzabal[2], Gustavo A. Echeverría[3], Gloria C. Valencia-Uribe[4], José M. Seco[2] and Delia B. Soria*[1]

[1]CEQUINOR (CONICET, CCT-La Plata), Departamento de Química, Facultad de Ciencias Exactas, Universidad Nacional de la Plata, 47 y 115 (1900). La Plata (Argentina). soria@quimica.unlp.edu.ar, http://cequinor.quimica.unlp.edu.ar
[2]Departamento de Química Aplicada Facultad de Química, UPV/EHU Paseo Manuel de Lardizábal 3, 20018 Donostia-San Sebastián (Spain).
[3]IFLP (CONICET, CCT-La Plata), Departamento de Física. Facultad de Ciencias Exactas, Universidad Nacional de La Plata (1900) La Plata (Argentina).
[4]GIAFOT, Departamento de Química, Facultad de Ciencias, Universidad Nacional de Colombia-Sede Medellín, Calle 59 A No. 63-020, Medellín (Colombia).

ABSTRACT

The already reported monomeric complex $Co(SDZ)_2bpy$ (**1**) and the novel ternary complex $Co(SDZ)_2(6MQ)_2$ (**2**) (SDZ = sulfadiazine; bpy = 2,2′-bipyridine and 6MQ = 6-methoxyquinoline) have been synthesized in order to study their magnetic properties. X-ray diffraction method indicates that in both compounds the SDZ acts as a bidentate ligand coordinating through the sulfonamide and the pyrimidinic N-atoms giving raise a CoN_6 coordination sphere. The complexes have been characterized based on elemental analyses, FTIR, UV-Visible spectroscopy and thermogravimetric analysis (TGA, only for 2). Both compounds, **1** and **2**, have been characterized magnetically and they show slow relaxation of the magnetization below 9 and 6 K, respectively.

Keywords – sulfadiazine, slow relaxation of the magnetization, single-ion magnets, Co (II) complexes, X-Ray structure.

1. Introduction

Since the discovery of single-molecule magnets (SMMs), molecular magnets that exhibit slow relaxation of the magnetization and magnetic hysteresis below the so-called blocking temperature (T_B), there has been a crescent interest in understanding the magnetic properties of mono and polynuclear coordination compounds. [1] The SMM behavior comes from the existence of an energy barrier (U) that prevents reversal of the molecular magnetization at low temperatures, which depends on the high ground spin state (S_T) and magnetic anisotropy of the entire molecule ($U = |D|\cdot S^2$ for integer S and $U = |D|\cdot(S^2-1/4)$ for non-integer S).[1b] Earliest attempts to enhance U consisted on increasing the total spin, which was achieved by increasing the number of ferromagnetically coupled metal centers. However, the control of the total anisotropy in polymetallic systems was extremely difficult and the increase in S led to a decrease in the magnetic

anisotropy in most cases. [2] In view of this, in the last years a new class of SMMs has emerged, named single-ion magnets (SIMs), where only a paramagnetic center is present and is responsible for SMM-like behavior. [3] Although the majority of the reported SMMs (mono and polynuclear) are lanthanide-based coordination compounds, [4] the search for new SIMs has been extended to transition metals complexes, for example Fe(II), [5] Co(II), [6] Ni(II) [7] and Mn(II) [8]. Despite the impressive values of the relaxation barrier observed in mononuclear transition-metal complexes (as high as 226 cm^{-1} for an Fe(I) complex, with a T_B = 4.5 K), [9] further improvement of their SIM properties is still required.

Co(II) complexes are good candidates for the construction of SIMs due to their large magnetic anisotropy, which arises from the significant orbital contribution to the total magnetic moment. [10] The magnetic properties of these complexes are greatly influenced by the coordination environments of Co(II) ions. For example, distorted octahedral Co(II) compounds can exhibit positive axial magnetic anisotropy (D > 0) and field-induced slow relaxation of the magnetization. [11] Trigonal prismatic coordination geometries, in contrast, lead to high negative values of D and therefore, they are very appropriate for the preparation of SIMs. [12] In fact, although the highest effective energy barrier exhibited by a Co(II) complex has been observed in a tetrahedral compound (U_{eff} = 118 cm^{-1} at zero *dc* field), [13] trigonal prismatic Co(II) complexes have also showed interesting SMM properties.

In addition to the coordination geometry, the coordinated ligands also influence the sign and magnitude of the magnetic anisotropy, thereby modulating the corresponding magnetic dynamics. The ligands chosen for this work are sulfonamides, which have been used as antibacterial for a long time. The metallic complexation of this family of compounds has brought to the sight a very wide range of biological properties, as well as magnetic properties. We have previously reported the structure and physicochemical characterization of some metal complexes of sulfonamides with different metals. [14] Recently, we have also reported the study of the aquatic toxicity, antimicrobial activities and cytotoxicity study in osteoblast-like cells in a cobalt complex with sulfaquinoxaline and 2,2′-Bipyrimidine as ligands. [15] Other similar complexes with sulfadiazine and sulfamethazine have also been reported. [16]

Relative to the 6MQ ligand, Cu(II), Ni(II), Zn(II) [17] and Hg(II) complexes with 6MQ as ligand were reported, but only the crystal structure of the compound containing mercury was discussed. [18] With the aim of expanding the previously mentioned studies and to study the effect of different coordination geometries in the magnetic properties of Co(II) compounds, two ternary complexes of Co(II) with SDZ and 2,2′-bipyridine or 6-methoxyquinoline as ligands have been prepared, $[Co(SDZ)_2bpy]$ (**1**) and $[Co(SDZ)_2(6MQ)_2]$ (**2**). The crystal structure of **1** was already published, but its magnetic properties were not studied. [19] The characterization of complex **2** by means of X-ray diffraction, thermogravimetry, FTIR and UV–Vis spectroscopies is also discussed.

2. Results and discussion

Although the crystal structure of complex **1** has already been published, structural features of this compound will be described in detail to understand the magnetic properties. The description will be based on our crystal data (CCDC 1430627).

2.1. Structure

Figure 1 and 2 show the coordination sphere of each metal center bonded to the ligands together with the used scheme label. In both cases, the Co(II) ion exhibits a CoN_6 coordination sphere. Calculation of the degree of distortion of the CoN_6 coordination polyhedra with respect to five ideal six-vertex polyhedra with the help of the SHAPE software [20] indicates that compound **1** is closer in shape to the trigonal prism (TPR-6) geometry, while **2** fits in better way to the octahedron (OC-6) one. For **1** values of 9.285 and 4.642 were calculated, while for **2** the calculation led to values of 4.174 and 16.804, for the OC-6 and the TPR-6 polyhedra, respectively (see table S1 in the Supporting Information).

Table 1 collects the experimental bond distances and angles around the cobalt atom determined by XRD for complexes **1** and **2**. For **1** the coordination sphere of the Co(II) cation consists of the bpy Nitrogen atoms at a distance of 2.137 (2) and 2.112 (2) Å and four nitrogen atoms from two SDZ molecules at 2.195(2) and 2.22(2) Å distances, completing the trigonal prism geometry. In the case of **2**, the Co(II) atom is located on an inversion center octahedrally coordinated by six nitrogen atoms. In the axial positions are located two 6MQ at Co–N110 distance of 2.209 (2) Å and four equatorial SDZ nitrogen atoms (Co–N27 2.222(2) Å and Co–N21 2.100(2) Å). The fact that the Co(II) atom is located at an inversion center, makes equivalent the two 6MQ and the SDZ ligands.

Furthermore, the lattice of both complexes is stabilized by the presence of intermolecular hydrogen bonds (see table S2 in the ESI). Besides, the 3D structure of **1** displays intermolecular π···π aniline-aniline (4.000 (2) Å) and bpy-bpy interactions (4.258 (2) Å) (Figure S1, ESI). In **2**, π···π interactions were observed between the quinolinic (3.931 (4) Å; see fig S1 in the ESI) and the pyrimidinyl rings of adjacent molecules (3.719 (3) Å).

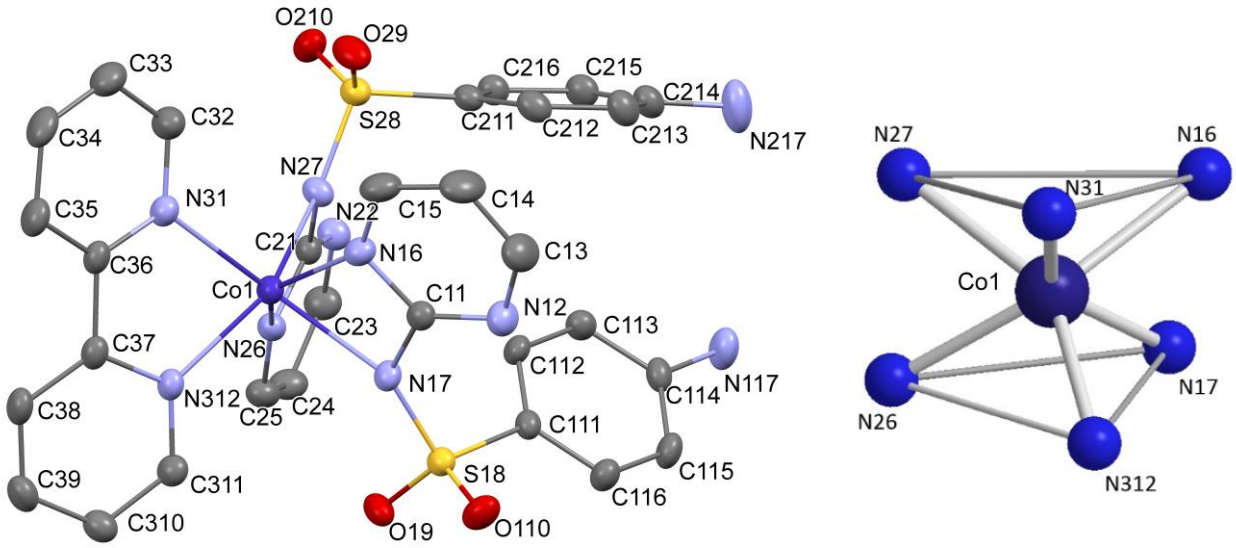

Figure 1. Left: Perspective view of complex **1** with displacement ellipsoids at the 50% probability level. Hydrogen atoms have been omitted for the sake of clarity. Right: Trigonal prismatic CoN_6 coordination sphere in **1**.

Table 1. Selected bond lengths (Å) and angles (°).

Complex **1**			
Co–N26	2.137 (1)	N26–Co–N27	61.58 (1)
Co–N27	2.198 (1)	N31–Co–N312	76.30 (1)
Co–N31	2.138 (1)	C211–S28–N27	108.42 (1)
Co–N312	2.112 (1)	C111–S18–N17	107.72 (1)
Co–N17	2.223 (1)		
Co–N16	2.153 (1)	N31–C36–C37–N312	15.26 (1)
S28–N27	1.616 (1)		
Complex **2**			
Co–N21	2.100 (2)	N21–Co1–N27	61.99 (1)
Co–N27	2.222 (2)	N21–Co1–N27’	118.01 (1)
Co–N110	2.209 (2)	C211–S28–N27	108.63 (1)
S28–N27	1.611 (1)		

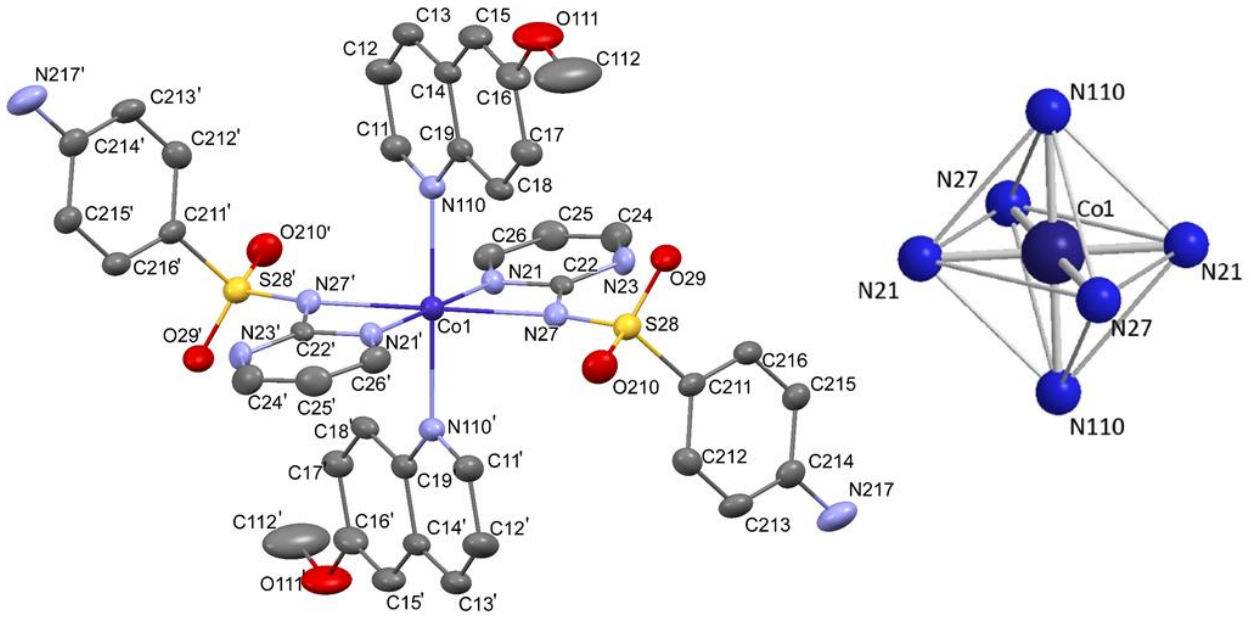

Figure 2. Left: Coordination sphere of complex **2** with displacement ellipsoids at the 30% probability level (H-atoms are omitted for clarity). Right: Distorted octahedron CoN_6 coordination sphere.

2.2. Magnetic Properties

The temperature dependence of $\chi_M T$ for complexes **1** and **2** were measured in an applied field of 0.1 T and are displayed in Figure 3. The $\chi_M T$ values at room temperature of 2.78 and 2.96 $cm^3 \cdot K \cdot mol^{-1}$, respectively for **1** and **2**, fall within the expected range for high spin d^7 Co(II) ions (S = 3/2). [21] Upon cooling, the $\chi_M T$ product of complex **1** remains almost constant until around 150 K and then starts decreasing to reach a value of 2.06 $cm^3 \cdot K \cdot mol^{-1}$ at 4.5 K. On the other hand, the $\chi_M T$ product of complex **2** decreases in the whole temperature range, reaching a value of 1.91 $cm^3 \cdot K \cdot mol^{-1}$ at 4.5 K. The observed behavior is most likely due to spin-orbit coupling effects, but it could also be due to intermolecular antiferromagnetic interactions.

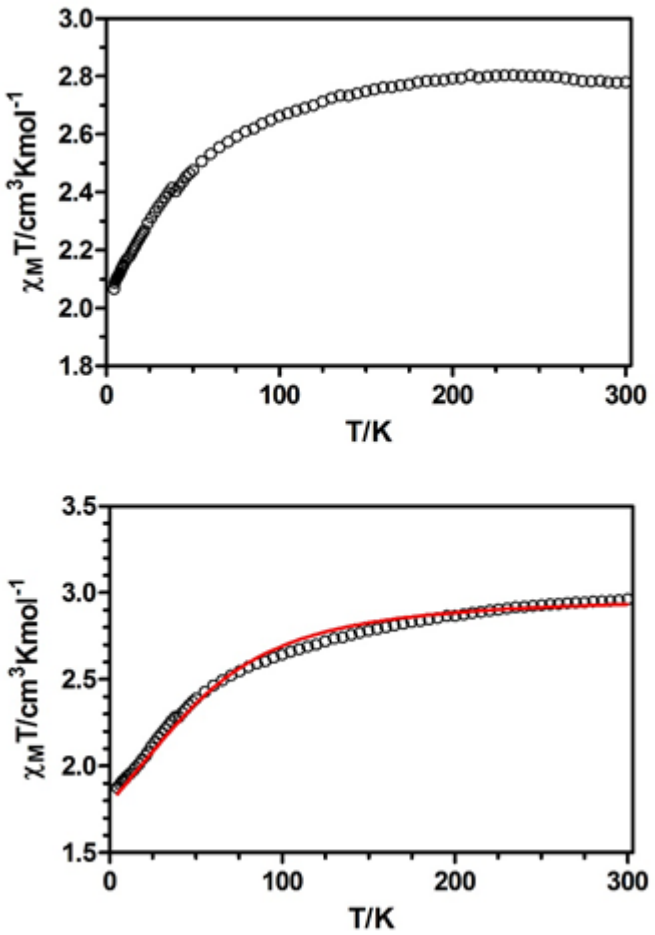

Figure 3. Variable-temperature magnetic susceptibility data for complexes **1** (top) and **2** (bottom). The red solid line is generated from the best fit to the following Hamiltonian: $H = D[S_z^2 - S(S+1)/3] + g_e\mu_B SH$.

In order to determine the magnitude and sign of the anisotropy parameter (D), isofield magnetization measurements were performed (Figure 4). The magnetization curves for complex **1** are almost superimposable, which has been typically related to the absence of anisotropy. However, it has been seen in bibliography that highly anisotropic systems can also lead to the same results. [8, 11d] All efforts to extract the value of the anisotropy parameter from these curves were unfruitful. Regarding complex **2**, the magnetization data at different fields (0-9 T) and temperatures (2-7 K) were analyzed simultaneously to the following Hamiltonian using the PHI program: [22]

$$H = D\left[S_z^2 - S(S+1)/3\right] + E\left(S_x^2 - S_y^2\right) + g_e\mu_B SH \qquad \text{(Equation 1)}$$

where S is the spin ground state, D and E are the axial and transverse magnetic anisotropies, respectively, μ_B is the Bohr magneton and H the applied magnetic field. The best fit of the data led to different sets of parameters: D = -81.6 cm^{-1}, E = 1.99 cm^{-1}, g = 2.78 and D = +81.1 cm^{-1}, E = 2.01 cm^{-1}, g = 2.78, which differ in the sign of D. The fit of the susceptibility data of **2** led to similar values, D = |78.9| cm^{-1} and g = 2.54, thus confirming the magnitude of D (Figure 3). However, it was impossible to unequivocally know the sign of D from the magnetic data.

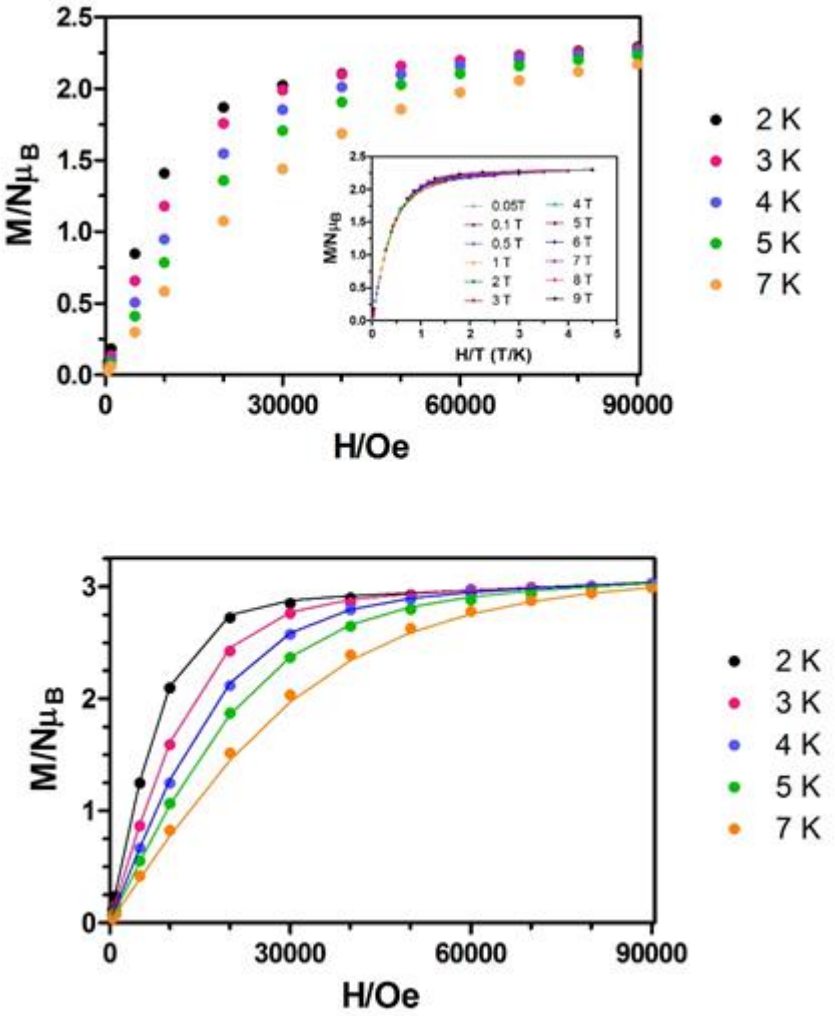

Figure 4. M vs H plots for **1** (top) and **2** (bottom) at different temperatures. Solid points represent the experimental data while the lines are generated connecting the data obtained with the PHI program for the indicated Hamiltonian and parameters. Inset: M vs H/T plot for **1**. Solid lines are only a guide for the eye.

With the aim of knowing if these compounds show slow relaxation of the magnetization or not, dynamic alternating-current (ac), magnetic measurements were performed as a function of both, temperature and frequency (Figures 5 and 6 and Figure S2). Despite the expected large anisotropy of the Co(II) ions, these complexes did not show any out-of-phase χ''_M signal under zero external field, which may be due to the fast resonant zero field quantum tunneling of the magnetization (QTM) through degenerate energy levels. This QTM relaxation process is forbidden for Kramers doublets such as Co(II) ions (the zero-field tunnel splitting is zero), but could be turned on by dipolar effects and hyperfine interactions. When the ac measurements were performed in the presence of a small external dc field of 1000 Oe to fully or partly suppress the QTM relaxation process, compounds **1** and **2** showed slow relaxation of the magnetization below 9 and 6 K, respectively.

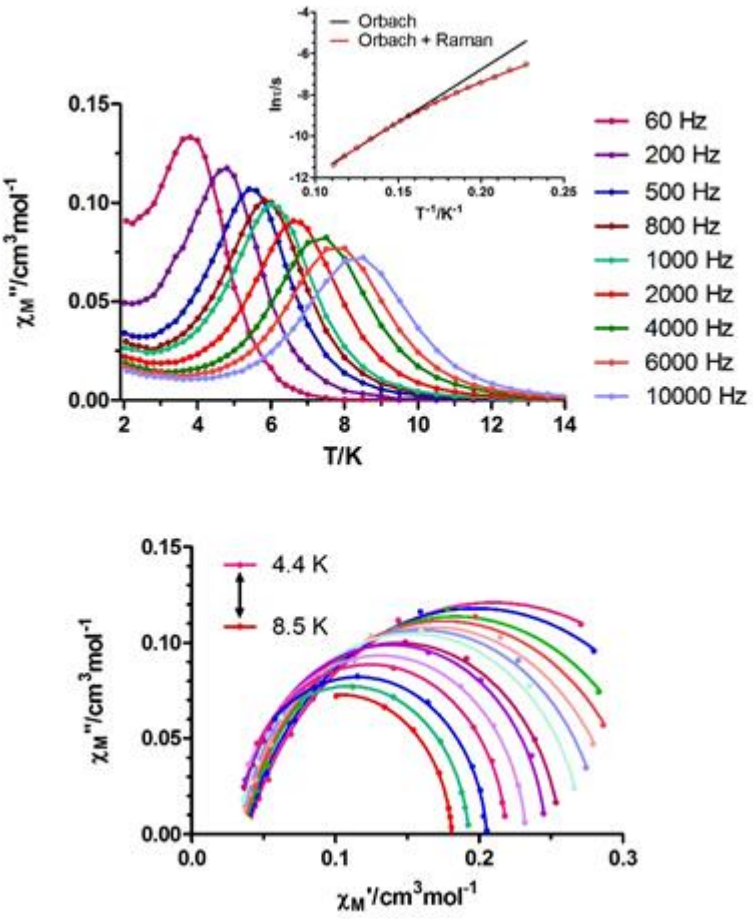

Figure 5. Top: Temperature dependence of the molar out-of-phase ac magnetic susceptibility (χ''_M) for **1** under an applied field of H_{dc} = 1000 Oe at different frequencies. Inset: Arrhenius plot (black lines) for the relaxation times. The red line corresponds to the best fit to Orbach plus Raman processes. Bottom: Cole-Cole plots. Solid lines represent the best fit of the experimental data to the generalized Debye model.

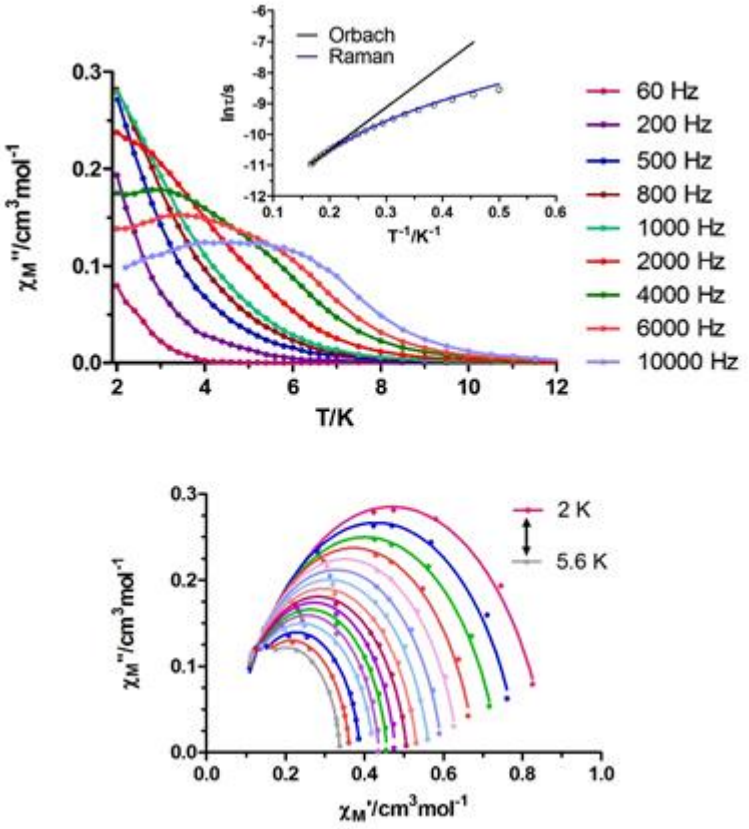

Figure 6. Top: Temperature dependence of the molar out-of-phase ac magnetic susceptibility (χ''_M) for **2** under an applied field of H_{dc} = 1000 Oe at different frequencies. Inset: Arrhenius plot (black lines) for the relaxation times. The blue line corresponds to the best fit to the Raman process. Bottom: Cole-Cole plots. Solid lines represent the best fit of the experimental data to the generalized Debye model.

The relaxation times (τ) were extracted from the fit of the frequency dependence of χ''_M at each temperature to the generalized Debye model (Figures 5 and 6, insets and Table S3). The fit of the linear portions of the data afforded effective energy barriers for the reversal of the magnetization of 50.6 K (35.2 cm^{-1}) and 13.7 K (7.0 cm^{-1}) with τ_0 values of $4.61 \cdot 10^{-8}$ s and $1.79 \cdot 10^{-6}$ s, respectively for **1** and **2**. As expected, the Arrhenius plots constructed from the temperatures and frequencies of the maxima observed for the χ''_M lead to similar results. For complex **1**, the χ''_M signals do not go to zero below the maxima; they increase up to 2 K, which indicates that the QTM process has not been fully eliminated.

The Cole-Cole diagrams for both compounds exhibit semicircular shapes that can be fitted by using the generalized Debye model (Figures 5 and 6). This fit provides a value for the α parameter, which is related to the width of the distribution of relaxation times, so that α = 1 corresponds to an infinitely wide distribution of relaxation times, whereas α = 0 represents a relaxation with a single time constant. The obtained α values in the range 0.22 (4.4 K) – 0.04 (8.5 K) and 0.21 (2 K) – 0.06 (5.6 K), respectively for **1** and **2**, suggest the existence of multiple relaxation processes (Table S3). In view of this, the experimental relaxation times were fitted to equations that take into account the

presence of different relaxation times. Although QTM is not fully suppressed in complex **1**, the best fit in the 4.4-8.5 K range was obtained considering both Orbach and Raman processes (Equation 2) and led to the following set of parameters: b = 0.067, n = 6.24, τ_0= 2.93·10^{-8} s and U_{eff}= 65.4 K.

$$\tau^{-1} = bT^n + \tau_0^{-1}\exp(-U_{eff}/k_BT) \qquad \text{(Equation 2)}$$

For complex **2**, the obtained energy barrier of 13.7 K is much lower than the expected value from the energy gap between the *Ms* = ± 1/2 and *Ms* = ± 3/2 levels (energy gap = 2*D* = 162 cm^{-1} = 233 K), which indicates that the relaxation cannot take place through an Orbach mechanism. The relaxation times were fitted to the Raman process (equation 3) and following recent works, [23] the simultaneous presence of direct and Raman processes was also considered (equation 4). The best fitting parameters were: b = 857.1 and n = 2.339 for equation 3 (Figure 6) and a = 1607, b = 297 and n = 2.84 for equation 4. In general, n=9 is expected for Kramers ions, [24] but depending on the structure of the levels, n values between 1 and 6 can be considered as reasonable. [25]

$$\tau^{-1} = bT^n \qquad \text{(Equation 3)}$$

$$\tau^{-1} = aT + bT^n \qquad \text{(Equation 4)}$$

The obtained energy barrier values fall within the range of experimental values observed for octahedral and trigonal prismatic Co(II) SIMs (Table S4). [11], [12], [26] It is interesting to note that all the octahedral Co(II) ions, independently of the sign of D, need a static external field to show SIM behavior. The large magnetic anisotropy of the octahedral Co(II) ions usually leads to Kramers ground doublets that are well separated from the first excited states, with energy gaps larger than typical acoustic phonon energies (the Orbach mode is therefore hindered). The spin-relaxation of these complexes has been usually explained by an admixture of single phonon direct processes and optical acoustic Raman-like processes, like in complex **2**. In these cases, the hyperfine interactions open paths for magnetic relaxation that would otherwise be forbidden by time reversal symmetry (direct processes), but they mask relaxation phenomenon at zero field. [23] On the other hand, for trigonal prismatic Co(II) SIMs, several relaxation modes such as Orbach, Raman and QTM have been admitted. [12d]

2.3 Electronic Spectroscopy

The UV-Vis spectra of the complexes were recorded in aqueous solution. The nature of the d-d metal transitions was studied by analyzing the visible diffuse reflectance (V-DR) of the complexes (Figures S3 and S4). In the 190 – 340nm spectral range, the UV-Vis spectrum of **1** displays bands at 240, 254, 292 and 304nm (ε =5.3·10^4, 5.3·10^4, 2.6·10^4 and 1.9·10^4 M^{-1}cm^{-1},

respectively), while the spectrum of **2** shows features at 202, 228, 260 and 326nm ($\varepsilon = 1.7 \cdot 10^5$, $1.2 \cdot 10^5$, $4.4 \cdot 10^4$ and $2 \cdot 10^4$ $M^{-1}cm^{-1}$, respectively). In both cases the bands observed at lower than 340nm are assigned to intraligand π-π* transitions. The V-DR of **1** shows two bands at 482 and 540 nm, which may tentatively be assigned to $^4T_{1g}(F) \rightarrow {}^4T_{1g}(P)$ and $^4T_{1g}(F) \rightarrow {}^4A_{2g}$ transitions, respectively. For the compound **2** the V-DR exhibits only one broad band centered at 490nm, assignable to the $^4T_{1g}$ (F) $\rightarrow {}^4T_{1g}$ (P) transition. These bands are in agreement with the partially allowed d-d transitions of the d^7 six-coordinated Co (II) complexes. [27]

2.4. Thermogravimetric Analysis

The analysis of TG and DTG curves of **2** indicates decomposition in three steps (Figure S5). The first one (142.0 ºC) corresponds to a weight loss of 34.7% consistent with the evolution of the two 6MQ ligands (loss of weight calculated 36.4%). The second step (282.1 ºC) observed in TG curve is compatible with a weight loss of 21.1 % and might be attributed to the decomposition of the anilinic group of the two SDZ (calculated 21.3%). The last incomplete step (419.2 ºC) probably corresponds to the decomposition of the remaining organic groups; loss of weight observed 31.43% (calculated 35.8%). The decomposition process yields cobalt monoxide as the final residue, as suggested by its FTIR spectra.

CONCLUSIONS

Two single-ion magnets based on Cobalt (II) with sulfadiazine and 2,2′-bipyridine (**1**) or 6-methoxyquinoline (**2**) have been synthesized. X-ray diffraction method indicates that the sulfadiazine (SDZ) acts as a bidentate ligand coordinating through the sulfonamide and the pyrimidinic N-atoms giving rise to a CoN_6 coordination sphere. The lattice in both compounds is stabilized by the presence of intermolecular hydrogen bonds and π···π interactions. Magnetic studies have showed slow relaxation of the magnetization below 9 and 6 K, respectively.

3. Experimental

3.1. Synthesis of the complexes

*Synthesis of **1** – [Co(SDZ)$_2$bpy]*

Complex **1** was prepared following a different synthesis compared with that previously reported [19]. The compound was obtained by direct reaction of ethanolic solutions of sulfadiazine sodium salt (NaSDZ), bpy and $CoCl_2 \cdot 6H_2O$ in 1:1:1 molar ratio. An orange precipitate was separated by centrifugation, washed several times with ethanol and its elemental microanalysis was performed. The slow evaporation of the mother solution provided well-developed orange crystals, which showed that the obtained compound was already reported. [19] Analytical calculation for

$CoC_{30}H_{26}N_{10}O_4S_2$: C, 50.49%; H, 3.67%; N, 19.63%; S, 8.97%. Found: C, 50.59%; H, 3.61%; N, 19.51%; S, 8.846%. The yield was 81.4%. FT-IR data (cm^{-1}): υ_{as} (NH_2) 3417, υ_s (NH_2) 3350 and 3320, υ (C=N and C=C) 1652 to 1549, υ_{as} (SO_2) 1325 and 1296, υ_s (SO_2) 1142 and 1135, υ (CoN) 412.

*Synthesis of **2** – [Co(SDZ)$_2$(6MQ)$_2$]*

The complex was prepared by adding methanolic solutions of NaSDZ (0.75mmol) and 6MQ (1.75mmol) to a methanolic solution containing $CoSO_4 \cdot 7H_2O$ (0.75mmol). The reaction was refluxed for 4 h and then, the resulting light orange solid was filtered, washed several times with methanol and subjected to elemental microanalysis. Mother solution was allowed to stand at room temperature and after slow evaporation, light orange crystals suitable for X-ray diffraction appeared. Analytical calculation for $CoC_{40}H_{28}N_{10}O_6S_2$: C, 54.73%; H, 4.36%; N, 15.96%; S, 7.31%. Found: C, 54.34%; H, 4.21%; N, 15.90%; S, 7.192%. The yield of the synthesis was 89.1%. FT-IR data (cm^{-1}): υ_{as} (NH_2) 3454, υ_s (NH_2) 3348, υ (C=N and C=C) 1635 to 1500, υ_{as} (SO_2) 1320, υ_s (SO_2) 1130.

3.2. Materials and methods

The FTIR spectra were carried out with an EQUINOX 55 spectrophotometer, in the range from 4000 to 400 cm^{-1} using the KBr pellet technique, with a spectral resolution of 4 cm^{-1}. Elemental (C, H, N and S) analyses were performed on a Leco CHNS-932 microanalyzer. The UV-Vis spectra were measured on aqueous solutions (10 μM), using a Hewlett–Packard 8452-A diode array spectrophotometer. The Vis-Diffuse reflectance spectra were recorded with MgO as reference with the help of a Shimadzu UV300 spectrophotometer. Variable-temperature magnetic susceptibility (4.5–300 K) measurements were carried out with a Quantum Design SQUID MPMS-7 T device. Magnetization measurements at different temperatures and magnetic fields and alternating current magnetic measurements (oscillating ac field of 3.5 Oe) were performed on a PPMS 6000 (Physical Property Measurement System) magnetometer. Thermogravimetric measurements were performed using a Shimadzu TGA-50 unit at a heating rate of 5°C/min. and nitrogen flow of 50 ml/min.

3.2.2 X-ray diffraction data

Data for complexes were collected on an Agilent Gemini Diffractometer with an EOS CCD detector equipped with a graphite-monochromated Mo Kα (λ= 0.71073 Å) radiation. X-ray diffraction intensities were collected (ω scans with θ and κ-offsets), integrated and scaled with CrysAlisPro [28] suite of programs. The unit cell parameters were obtained by least-squares refinement (based on the angular settings for all collected reflections with intensities larger than seven times the standard

deviation of measurement errors). Data were corrected empirically for absorption employing the multi-scan method implemented in CRYSALISPRO. The structures were solved by direct methods with SHELXS-97 [29] and the molecular models refined by full-matrix least-squares procedure on F^2 with SHELXL-97. [29] The hydrogen atoms were positioned stereo-chemically and refined with the riding model. All the attempts to recrystallize the compound 2 from different solvents and temperatures yielded crystals with two or more domains which produced X-ray data of limited quality as consequence. The best data were obtained from a crystal obtained from the mother solution of the reaction in methanol as previously described. Crystal data and refinement results are summarized in Table 2. CIF files with details of the crystal structures reported in this paper have been deposited with the Cambridge Crystallographic Data Centre, under deposition numbers CCDC1430627 (**1**) and 1430628 (**2**). The complementary structural data of complex 1 which had been published earlier by Ran et al. [19] can be found under CCDC 977532.

Table 2. Crystal data and structure refinement for complexes **1** and **2**.

Compound	**1**	**2**
Empiric formula	$CoC_{30}H_{26}N_{10}O_4S_2$	$CoC_{40}H_{28}N_{10}O_6S_2$
Formula weight	713.11	875.84
Temperature	293 K	293 K
Wavelength	0.71073 Å	0.71073 Å
Crystal system	Triclinic	Monoclinic
Space group	P-1	P 21/n
Unit Cell dimensions	a = 10.282 Å	a = 8.7968(8) Å
	b = 12.401 Å	b = 21.5595(15) Å
	c = 12.877 Å	c = 10.3300(8) Å
	α=75.50°	
	β = 82.31°	β =94.154(7)°
	γ = 73.52º	
Volume	1641.9 Å³	1955.55 Å³
Z, Density (calculated)	2, 1.558 g cm^{-3}	4, 1.489 g cm^{-3}
Absorption coefficient	0.758 mm^{-1}	0.609 mm^{-1}
F(000)	734	906
Crystal size	0.196 x 0.112 x 0.053 mm^3	0.331 x 0.216 x 0.053 mm^3
θ range for data collection	3.046 to 29.263º	3.087 to 25.996º
Index ranges	$-13 \le h \le 14$	$-7 \le h \le 10$
	$-16 \le k \le 17$	$-26 \le k \le 24$
	$-16 \le l \le 16$	$-12 \le l \le 9$
Reflections collected / unique	12325 / 6888 [R(int)=0.0293]	8679 / 3830 [R(int)=0.0631]
Completeness to θ = 25.242º	99.8 %	99.7 %
Absorption correction	Semi-empirical from equivalents	Semi-empirical from equivalents
Max. and min. transmission	1 and 0.96837	1 and 0.9174
Refinement method	Full-matrix least-squares on F2	Full-matrix least-squares on F2
Data/restraints/parameters	6888 / 22 / 512	3830 / 0 / 268

Goodness-of-fit on F2	0.959	1.254
Final R indices [I > 2σ(I)][a]	R1 = 0.0419, wR2 = 0.0924	R1 = 0.1081, wR2 = 0.1959
R indices (all data)[a]	R1 =0.0693, wR2 = 0.1071	R1 = 0.1527, wR2 = 0.2172
Largest diff. peak and hole	0.286 and -0.286 e.Å^{-3}	0.668 and -0.453 e.Å^{-3}

[a]$R1=\Sigma||F_o|-|F_c||/\Sigma|F_o|$, $wR2=[\Sigma w(|F_o|^2-|F_c|^2)^2/\Sigma w(|F_o|^2)^2]^{1/2}$

ACKNOWLEDGEMENTS

D.B.S., G.E. and C.V-P. thank to UNLP, CONICET and ANPCyT from Argentina for financial support. J.M.S. thanks to UPV/EHU. I.O. is also grateful to UPV/EHU for a postdoctoral grant. G.C.V.U. thanks to Universidad Nacional de Colombia. The authors thank for technical and human support provided by SGIker of UPV/EHU and European funding (ERDF and ESF).

Table of Contents

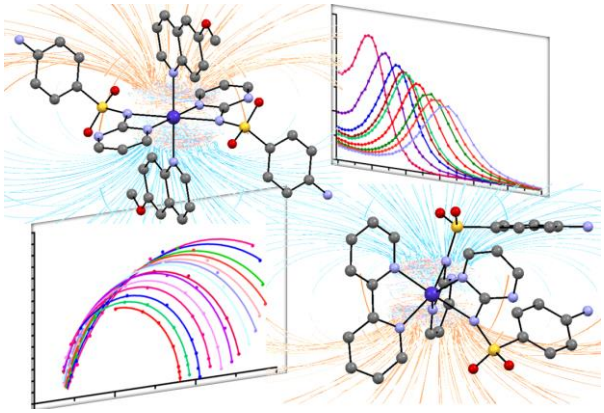

Two monomeric Cobalt complexes $Co(SDZ)_2bpy$ and $Co(SDZ)_2(6MQ)_2$ have been prepared and characterized. X-ray diffraction method indicates that in both compounds the sulfadiazine (SDZ) acts as a bidentate ligand coordinating through the sulfonamide and the pyrimidinic N-atoms. The complexes showed slow relaxation of the magnetization below 9 and 6 K.

REFERENCES

[1] a) R. Sessoli, D. Gatteschi, A. Caneschi, M. A. Novak, *Nature* **1993**, *365*, 141-143; b) D. Gatteschi, R. Sessoli and J. Villain, Molecular Nanomagnets, Oxford University Press, Oxford, U.K., 2006.

[2] F. Neese, D. A. Pantazis, *Faraday Discuss* **2011**, *148*, 229-238.

[3] a) D. N. Woodruff, R. E. P. Winpenny, R. A. Layfield, *Chem. Rev.* **2013**, *113*, 5110-5148;

b) A. K. Bara, C. Pichona, J.-P. Suttera, *Coord. Chem. Rev*. **2016**, *308*, 346-380; c) A. Grigoropoulos, M. Pissas, P. Papatolis, V. Psycharis, P. Kyritsis, Y. Sanakis, *Inorg. Chem.* **2013**, *52*, 12869-12871.

[4] a) J. D. Rinehart, M. Fang, W. J. Evans, J. R. Long, *J. Am. Chem. Soc*. **2011**, *133*, 14236-14239; b) R. J. Blagg, L. Ungur, F. Tuna, J. Speak, P. Comar, D. Collison, W. Wernsdorfer, E. J. L. McInnes, L. F. Chibotaru, R. E. P. Winpenny, *Nat. Chem.* **2013**, *5*, 673-678; c) C. R. Ganivet, B. Ballesteros, G. De La Torre, J. M. Clemente-Juan, E. Coronado and T. Torres, *Chem. - A Eur. J.* **2013**, *19*, 1457-1465; d) I. Oyarzabal, J. Ruiz, J. M. Seco, M. Evangelisti, A. Camón, E. Ruiz, D. Aravena, E. Colacio, *Chem. - A Eur. J*. **2014**, *20*, 14262-14269; e) J. D. Rinehart, M. Fang, W. J. Evans, J.R. Long, *Nat. Chem*. **2011**, *3*, 538-542.

[5] J. M. Zadrozny, M. Atanasov, A.M. Bryan, C.-Y. Lin, B.D. Rekken, P. P. Power, F. Neese, J. R. Long, *Chem. Sci*. **2013**, *4*, 125-130.

[6] a) T. Jurca, A. Farghal, P.-H. Lin, I. Korobkov, M. Murugesu, D. S. Richeson, *J. Am. Chem. Soc.* **2011**, *133*, 15814–15817; b) J. M. Zadrozny, J. R. Long, *J. Am. Chem. Soc.* **2011**, *133*, 20732–20734; c) A. Buchholz, A. O. Eseola, W. Plass, *C. R. Chimie* **2012**, *15*, 929-936; d) S. Ziegenbalg, D. Horning, H. Görls, W. Plass, *Inorg. Chem*. **2016**, *55*, 4047-4058.

[7] R. C. Poulten, M. J. Page, A. G. Algarra, J. J. Le Roy, I. López, E. Carter, A. Llobet, S. A. Macgregor, M. F. Mahon, D. M. Murphy, M. Murugesu, M. K. Whittlesey, *J. Am. Chem. Soc.* **2013**, *135*, 13640-13643.

[8] a) J. Vallejo, A. Pascual-Álvarez, J. Cano, I. Castro, M. Julve, F. Lloret, J. Krzystek, G. De Munno, D. Armentano, W. Wernsdorfer, R. Ruiz-García, E. Pardo, *Angew. Chem. Int. Ed*. **2013**, *52*, 14075-14079; b) R. Ishikawa, R. Miyamoto, H. Nojiri, B. K. Breedlove, M. Yamashita, *Inorg. Chem*. **2013**, *52*, 8300-8302.

[9] J. M. Zadrozny, D. J. Xiao, M. Atanasov, G. J. Long, F. Grandjean, F. Neese, J. R. Long, *Nat. Chem*. **2013**, *5*, 557-558.

[10] A. Palii, J. Clemente-Juan, E. Coronado, S. Klokishner, S. Ostrovsky, O. Reu, *Inorg. Chem.*, **2010**, *49*, 8073-8077.

[11] a) R. Herchel, L. Váhovská, I. Potočňák, Z. Trávníček, *Inorg. Chem*. **2014**, *53*, 5896-5898; b) J. Vallejo, I. Castro, R. Ruiz-García, J. Cano, M. Julve, F. Lloret, G. De Munno, W. Wernsdorfer, E. Pardo, *J. Am. Chem. Soc.* **2012**, *134*, 15704-15707; *c*) E. Colacio, J. Ruiz, E. Ruiz, E. Cremades, J. Krzystek, S. Carretta, J. Cano, T. Guidi, W. Wernsdorfer, E. K. Brechin, *Angew. Chem. Int. Ed*. **2013**, *52*, 9130-9134; *d*) D. Wu, X. Zhang, P. Huang, W. Huang, M. Ruan, Z. W. Ouyang, *Inorg. Chem*. **2013**, *52*, 10976-10982; e) S. Roy, I. Oyarzabal, J. Vallejo, J. Cano, E. Colacio, A. Bauza, A. Frontera, A. M. Kirillov, M. G. B. Drew, S. Das, *Inorg. Chem*. **2016**, doi: 10.1021/acs.inorgchem.6b01087.

[12] a) S. Gomez-Coca, E. Cremades, N. Aliaga-Alcalde and E. Ruiz, *J. Am. Chem. Soc*. **2013**, *135*, 7010-7018; b) Y.-Y. Zhu, C. Cui, Y.-Q. Zhang, J.-H. Jia, X. Guo, C. Gao, K. Qian, S.-D. Jiang, B.-W. Wang, Z.-M. Wanga, S. Gao, *Chem. Sci*. **2013**, *4*, 1802-1806; c) Y.-Y. Zhu, Y.-Q. Zhang, T.-T. Yin, C. Gao, B.-W. Wang, S. Gao, *Inorg. Chem*. **2015**, *54*, 5475-5486; d) V. V. Novikov, A. A. Pavlov, Y. V. Nelyubina, M.-E. Boulon, O. A. Varzatskii, Y. Z. Voloshin, R. E. P. Winpenny, *J. Am. Chem. Soc*. **2015**, *137*, 9792-9795.

[13] Y. Rechkemmer, F. D. Breitgoff, M. van der Meer, M. Atanasov, M. Hakl, M. Orlita, P. Neugebauer, F. Neese, B. Sarkar, J. van Slageren, *Nat. Comm*. **2016**, *7*, 10467.

[14] a) G. E. Camí, M. E. Chacón Villalba, P. Colinas, G. A. Echeverría, G. Estiu, D. B. Soria, *J. Mol. Struct.* **2012**, *1024*, 110-116; b) G. Estiu, M. E. Chacón Villalba, G. E. Camí, G. A. Echeverria, D. B. Soria, *J. Mol. Struct*. **2014**, *1062*, 82-88; c) G. Camí, E. Chacón Villalba, Y. Di Santi, P. Colinas, G. Estiu, D. B. Soria, *J. Mol. Struct*. **2011**, *995*, 72-77.

[15] C. Villa-Perez, J. F. Cadavid-Vargas, G. E. Camí, F. Giannini, M. E. Chacón Villalba, G. E. Echeverría, I. C. Ortega, G. C Valencia, S. B. Etcheverry, D. B. Soria, *Inorg. Chim. Acta* **2016**, *447*, 127-133.

[16] a) T.-J. He, Y.-S. Tan, Y.-Q. Gu, Z.-F. Chen, H. Liang, *Acta Crystallogr. Sect. E: Struct. Reports Online*, 2010, 66, 684-685; b) F. Öztürk, İ. Bulut, A. Bulut, *Spectrochim. Acta Part A Mol. Biomol. Spectrosc*. **2015**, *138*, 891-899.

[17] J. R. Allan, J. Dahyrnple, *Thermochim. Acta*. **1991**, *191*, 223-230.

[18] C. Villa-Pérez, I. C. Ortega, A. M. Payán-Aristizábal, G. Echeverría, G. C. Valencia-Uribe, D. B. Soria, *Zeitschrift Für Naturforsch. B.* **2015**, *70*, 719-725.

[19] F.-M. Ran, Y.-Y. Zhao, X.-H. Zhao, J. Zhang, J.-G. Pan, X. Li, *Chin. J. Inorg. Chem*. **2014**, *30*, 913-920.

[20] M. Llunell, D. Casanova, J. Cirera, J. M. Bofill, P. Alemany, S. Alvarez, M. Pinsky, D. Avnir, SHAPE v1.1b, Barcelona, 2005.

[21] a) R. Boča, *Coord. Chem. Rev*. **2004**, *248*, 757-815 and references cited therein; b) J. Titiš, R. Boča, *Inorg. Chem*., 2011, **50**, 11838-11845.

[22] N. F. Chilton, R. P. Anderson, L. D. Turner, A. Soncini, K. S. Murray, *J. Comput. Chem*. **2013**, *34*, 1164-1175.

[23] S. Gómez-Coca, A. Urtizberea, E. Cremades, P. J. Alonso, A. Camón, E. Ruiz, F. Luis, *Nat. Commun.* **2014**, *5*, 4300.

[24] A. Abragam and B. Bleaney, *Electron Paramagnetic Resonance of Transition Ions*, Clarendon Press. Oxford, 1970.

[25] K. N. Shrivastava, *Phys. Status Solidi B* **1983**, *117*, 437-458.

[26] a) C. Plenk, J. Krause, E. Rentschler, *Eur. J. Inorg. Chem*. **2015**, 370-374; b) V. Chandrasekhar, A. Dey, A. J. Mota, E. Colacio, *Inorg. Chem*. **2013**, *52*, 4554-4561.

[27] a) M. Gaber, K. Y. El-Baradie, *Chem. Pap*., **2003**, *57*, 317-321; b) L. Banci, A. Bencini, C. Benelli, D. Gatteschi, *Struct. Bond*. **1982**, 37-86.

[28] CrysAlis CCD, CrysAlis RED and associated programs: Oxford Diffraction program name(s)., 2006.

[29] G. M. Sheldrick, *Acta Crystallogr. A*. **2008**, *64*, 112-122.